Research Square

Preprints are preliminary reports that have not undergone peer review.
They should not be considered conclusive, used to inform clinical practice,
or referenced by the media as validated information.

Histological Characteristics and Molecular Regulatory Mechanisms Associated with Laying Performance and Egg Shape Traits in Huaixiang Chickens

ShouQuan Yang
Guangdong Ocean University
YinLin Yao
Guangdong Ocean University
XiaoWen Zeng
Guangdong Ocean University
QingZhuo li
Guangdong Ocean University
Li Zhang
Guangdong Ocean University
Jiang Wu
wujiang610@126.com
Guangdong Ocean University https://orcid.org/0000-0002-0771-1791

Research Article

Keywords: Huaixiang chicken, BMP15 gene, ZDHHC2 gene, laying rate, egg shape index

Posted Date: July 3rd, 2026

DOI: https://doi.org/10.21203/rs.3.rs-10061527/v1

License: This work is licensed under a Creative Commons Attribution 4.0 International License.
Read Full License

Abstract

The present study investigated the histological and molecular mechanisms underlying laying performance and egg shape traits in Huaixiang chickens. Thirty-six-week-old hens were classified according to laying rate and egg shape index. Follicular morphology, oviduct magnum histology, and the expression patterns of *BMP15* and *ZDHHC2* were analyzed. Significant structural differences in ovarian follicles were observed among laying groups. In large white follicles, hens with high laying performance exhibited relatively thinner and loosely arranged theca and granulosa cell layers, whereas low-laying hens showed thicker and denser cellular structures. In small yellow follicles, the low-laying group displayed a markedly thinner granulosa cell layer and a significantly increased theca-to-granulosa cell ratio compared with the high-laying group. *BMP15* expression increased with laying performance, with the most pronounced differences detected in small yellow follicles. Correlation analysis further demonstrated that *BMP15* expression was significantly positively associated with laying rate ($P < 0.01$). Distinct histological differences were also identified in the oviduct magnum among hens with different egg shape indices. The round-egg group showed more developed mucosal folds and glandular structures, whereas the elongated-egg group exhibited relatively loose tissue organization. In addition, *ZDHHC2* expression was significantly positively correlated with egg shape index ($P < 0.01$). These findings suggest that granulosa cell development and *BMP15* expression are closely related to laying performance, while magnum morphology and *ZDHHC2* expression may contribute to egg shape formation in Huaixiang chickens. This study provides a theoretical basis for understanding the regulation of reproductive and egg quality traits in poultry.

Introduction

Laying rate and egg shape are two important economic traits in poultry production that directly affect breeding efficiency, egg quality, and hatchability. Laying rate reflects the overall reproductive capacity of hens and is closely associated with ovarian follicular development, endocrine regulation, and ovulatory rhythm. Egg shape traits, particularly the egg shape index, influence not only external egg quality and commercial value but also eggshell strength, embryonic development, and hatching performance (Narushin and Romanov 2002). Previous studies demonstrated that an appropriate egg shape index contributed to improved gas exchange during incubation and enhanced embryonic survival (Robert 2004; Peşmen 2025). Therefore, elucidating the biological mechanisms underlying laying performance and egg shape formation remains essential for the genetic improvement and production optimization of indigenous chicken breeds such as Huaixiang chicken (Chen et al. 2023).

The ovary plays a central role in regulating laying performance through follicular recruitment, selection, maturation, and ovulation (Wang et al. 2023). During follicular development, granulosa cells and theca cells coordinately regulate steroid hormone synthesis and follicular growth (Rangel et al. 2014). Among the molecular regulators involved, bone morphogenetic protein 15 (*BMP15*), a member of the transforming growth factor-β (TGF-β) superfamily, is considered a key oocyte-derived factor that modulates granulosa cell proliferation, differentiation, and steroidogenesis through paracrine signaling

pathways (Moore and Shimasaki 2005). Previous studies showed that *BMP15* is closely associated with ovulation rate and reproductive performance, whereas aberrant expression impaired follicular development and ovulatory function. In poultry, *BMP15* expression exhibits dynamic changes throughout follicular development, particularly during the transition from small yellow follicles to hierarchical follicles. However, studies exploring the associations among *BMP15* expression, follicular morphology, and laying performance in indigenous chicken breeds remain scarce (Han et al. 2015).

Egg shape formation mainly depends on the coordinated functions of different regions of the oviduct (Mehta et al. 2005). The magnum is responsible for albumen secretion, the isthmus participates in eggshell membrane formation, and the uterus regulates eggshell mineralization (Mishra 2019). In addition, oviductal contraction rhythm, egg retention time, and secretory activity collectively influence final egg morphology. Accumulating evidence suggests that post-translational protein modifications play important roles in reproductive regulation. Among these modifications, protein palmitoylation affects protein localization, stability, and signal transduction. ZDHHC2, a representative palmitoyl transferase, plays important roles in regulating cell proliferation, differentiation, and secretion by catalyzing protein palmitoylation. In the oviduct magnum, the secretory activity of epithelial cells and tissue integrity directly influence albumen deposition and may consequently affect egg shape formation (Todireanu et al. 2014). Therefore, *ZDHHC2* is hypothesized to contribute to the maintenance of oviductal function and the regulation of egg shape traits through the modulation of secretion-related proteins and cytoskeletal dynamics. Nevertheless, studies investigating the role of *ZDHHC2* in the regulation of egg shape traits in poultry remain largely unexplored (Sah et al. 2021).

Collectively, systematic investigation of ovarian follicular development and oviductal functional regulation is crucial for understanding the mechanisms underlying laying performance and egg shape traits in poultry. Elucidating the functional roles of *BMP15* in follicular development and *ZDHHC2* in oviductal function is expected to provide important mechanistic insights into the molecular regulation of reproductive traits and offer a theoretical basis for molecular breeding and the improvement of productive performance in indigenous chicken breeds.

Materials and methods

Experimental Animals and Feeding

A total of 34 healthy 36-week-old Huaixiang laying hens (Gallus gallus domesticus) were used as experimental animals in this study. The experiment was conducted at the Experimental Animal Center of Huguang Campus, Guangdong Ocean University. Prior to the experiment, all hens underwent health screening to ensure the absence of obvious diseases or abnormal production performance. All experimental procedures involving animals were approved by the Institutional Animal Care and Use Committee (IACUC) of the College of Agriculture, Guangdong Ocean University (Approval No. GDOU-NXY-2024-016). A completely randomized design (CRD) was adopted for animal grouping, and all birds were managed under standardized batch-feeding conditions.

The experimental period lasted for 21 d. During the trial, all hens had ad libitum access to feed and water, with water continuously supplied through an automatic drinking system. The basal diet was formulated according to the NY/T 33-2004 Feeding Standard for Laying Hens and was moderately optimized based on the breed characteristics of Huaixiang chickens and the feed resource conditions in the Lingnan region (the detailed composition is shown in Table 1). Feeding and management practices were conducted in accordance with standardized commercial laying hen production procedures. The poultry house was maintained under good ventilation and hygienic conditions, and the health status of the birds was systematically monitored and recorded daily throughout the experimental period.

Table 1
Ingredient composition and nutrient content of the basal diet (Air-dried Basis)

Ingredients	***P*ercent (%)**	**Calculated nutrient levels[2]**	**Content (%)**
Corn	54.18	ME (MJ/kg)	13.68
Wheat bran	9.95	C*P*	20.04
Soybean meal	19.78	Ca	3.25
Fish meal	5.00	T*P*	0.58
Limestone	7.54	Met	0.62
$Na(HCO_3)$ [2]	2.45	Cys	0.41
NaCl	0.42	Lys	0.73
Premix[1]	0.68		

[1]Premix provided per kilogram of diet: VA 150000 U, VD 3300000 U, VE 61.7 mg, VK 3.5 mg, VBl 2.88 mg, VB2 9.5 mg, VB6 6.2 mg, VB12 0.03 mg, Fe 80 mg, Cu 2 mg, Zn 75 mg, Mn 62 mg, I 0.38 mg, Se 0.15 mg, niacin 60.5 mg, calcium *P*antothenate 17.5 mg, folic a cid 1.7 mg, biotin 0.36 mg, choline chloride 600 mg as well as antibacterial growth *P*romoter, antioxidant.

[2]Nutrient levels were analyzed values

Determination of Laying Rate and Grouping

At the beginning (D0) and the end (D21) of the experiment, all hens were weighed after fasting before the morning feeding, with a measurement accuracy of 0.1 g. To minimize the influence of flock size differences on the evaluation of production performance, the number of eggs produced by each hen was recorded daily throughout the experimental period, and the individual laying rate was calculated. The formula was as follows:

$$\text{Individual Laying Rate}\,(\%) = \frac{\text{Number of Laying Days per Hen}}{\text{Total Experimental Days}} \times \ 100$$

At the end of the experiment, the laying rate data of all individuals were ranked in descending order, and hens were grouped based on their distribution characteristics. A quantile-based grouping method was applied to divide the population into high-, medium-, and low-laying groups. During the grouping process, sample sizes were kept as balanced as possible among groups, while also ensuring sufficient phenotypic differentiation between groups.

Determination and Grouping of Egg Shape Index

During the experimental period, all eggs produced by each hen were collected, and egg shape index was measured on an individual basis. The longitudinal diameter (length) and transverse diameter (width) of each egg were measured using a digital vernier caliper with a precision of 0.02 mm. Each egg was measured three times for both length and width, and the average values were used for calculation. The egg shape index (SI) was calculated using the following formula:

$$\text{Egg Shape Index}\ \ (\%) = \frac{\text{Longitudinal Diameter}}{\text{Transverse Diameter}} \times \ 100$$

To improve the representativeness of the measurements, multiple eggs produced by each hen during the experimental period were repeatedly measured, and the mean value was used as the individual egg shape index.

Based on the distribution characteristics of egg shape index and with reference to the “NY/T 823–2020 Egg Quality Grading Standard,” the experimental population was further classified into groups. Specifically, hens with an egg shape index > 75% were defined as the round-egg group, those with 70% – 75% were defined as the standard-egg group, and those with < 70% were defined as the elongated-egg group. During grouping, efforts were made to maintain relatively balanced sample sizes among groups while maximizing phenotypic differences between groups, thereby facilitating subsequent histological observation and gene expression analysis.

Tissue Collection and Processing

At the end of the experiment, all hens were sampled uniformly after an overnight fast. Birds were humanely euthanized by carotid artery exsanguination in accordance with animal welfare guidelines. Under sterile conditions, the abdominal cavity was rapidly opened, and the ovary and oviduct magnum were collected. Large white follicles (LWF) and small yellow follicles (SYF) were isolated according to follicular diameter and color characteristics, while oviductal tissue was obtained from the magnum region.

All samples were rinsed with pre-cooled phosphate-buffered saline (PBS) to remove residual blood and impurities, then cut into approximately 0.5 cm^3 sections and processed according to subsequent experimental requirements. For histological analysis, tissues were fixed in 4% paraformaldehyde at 4°C for 12–24 h, followed by paraffin embedding and hematoxylin–eosin (HE) staining. For gene expression analysis, tissues were transferred into RNase-free tubes containing RNAlater solution, temporarily stored at 4°C, and subsequently preserved at − 80°C until RNA extraction and RT-PCR analysis. All procedures were conducted rapidly under low-temperature and RNase-free conditions to preserve tissue morphology and RNA integrity.

Histological Observation and Morphological Analysis

Paraffin-embedded ovary and oviduct magnum tissues were sectioned at 4–5 μm thickness. Sections were mounted on glass slides, dried at 60°C for 2 h, deparaffinized in xylene, and rehydrated through a graded ethanol series to distilled water. Hematoxylin–eosin (HE) staining was subsequently performed. Briefly, sections were stained with hematoxylin for 5–8 min, differentiated with 1% acid alcohol, blued under running water, and counterstained with eosin for 1–3 min. After staining, sections were dehydrated through graded ethanol, cleared in xylene, and sealed with neutral resin. Prepared slides were observed under a light microscope (Olympus BX51, Japan), and representative images were captured at a uniform magnification for subsequent histomorphological analysis.

Primer Design

Based on gene sequence information of Gallus gallus retrieved from the NCBI database, gene-specific primers for the candidate genes *ZDHHC2* and *BMP15* were designed using Primer 5.0 software. During primer design, exon–exon spanning regions were preferentially selected to minimize amplification from genomic DNA. Primer specificity was further verified using BLAST alignment analysis. The primer sequences and related information are listed in Table 2.

In this study, *β-actin* was used as the internal reference gene to normalize expression differences among samples. All primers were synthesized by TransGen Biotech Co., Ltd. (Beijing, China) and purified by HPLC prior to use.

Table 2
Primer sequences used for Semi-quantitation RT-*P*CR

Primer name	GenBank accession	Primer Sequence (5'-3')	Product Size (b*P*)
ZDHHC2	XM_046940370.1	F^2: AAGTCTTACGGCGAGCAG	232
		R^2: GAACAGTGATGGCAACG	
BMP15	NM_001006589	F: GTAGCGTGGGTTGTAGCGATGG	253
		R: CCTCCTCTTCCTCAATGACACC	
β-actin	NM_205518.2	F: GTGATGAAGCCCAGAGCAAA	116
		R: TACGACCAGAGGCATACAGG	

RNA Extraction and Semi-quantitative RT-PCR

Total RNA was extracted using TRIzol reagent (Invitrogen) according to the manufacturer's instructions. RNA concentration and purity were determined using a microspectrophotometer (OD260/OD280), and RNA integrity was verified by 1% agarose gel electrophoresis. First-strand cDNA was synthesized from total RNA using a commercial reverse transcription kit following the manufacturer's protocol, and the resulting cDNA was stored at − 20°C for subsequent analyses.

Semi-quantitative RT-PCR was performed to assess the expression of target and reference genes. The reaction mixture consisted of cDNA template, gene-specific primers, 2× PCR Master Mix, and RNase-free water. The PCR program included initial denaturation at 95°C for 3–5 min, followed by 30–35 cycles of denaturation at 95°C for 30 s, optimized annealing temperature for 30 s, and extension at 72°C for 30–60 s, with a final extension at 72°C for 5–10 min. Amplified products were separated on 1.5% agarose gels and visualized using a gel imaging system. Band intensities were quantified using ImageJ software, and relative gene expression levels were calculated as the ratio of target gene intensity to that of the internal reference gene *β-actin*.

Statistical Analysis

All experimental data in this study were statistically analyzed using SPSS (version 26.0, IBM Corp., USA) and GraphPad Prism (version 10.0). Prior to statistical analysis, all data were subjected to normality testing using the Shapiro–Wilk test and homogeneity of variance testing using Levene's test to verify whether the assumptions for parametric analysis were satisfied. For data exhibiting normal distribution and homogeneity of variance, differences among groups were analyzed by one-way analysis of variance (one-way ANOVA). When significant differences were detected, Duncan's multiple range test or Tukey's post hoc test was further performed for multiple comparisons among groups. Data that did not meet the assumptions of normal distribution were analyzed using nonparametric tests, such as the Kruskal–Wallis H test. Pearson correlation analysis was performed to evaluate linear relationships among

variables. All results are presented as mean ± standard error of the mean (Mean ± SEM). Statistical significance was defined as $P < 0.05$, whereas $P < 0.01$ was considered highly significant.

Results

Phenotypic variation in laying rate among Huaixiang chickens

The 34 experimental Huaixiang chickens were ranked according to laying rate from high to low and subsequently divided into groups, as shown in Fig. 1. The results indicated significant differences in laying rate among groups with different production levels ($P < 0.05$). Multiple comparison analysis further revealed extremely significant differences in laying rate among the high-, medium-, and low-laying groups ($P < 0.0001$). Under identical feeding and environmental conditions, substantial individual variation in laying performance was observed among Huaixiang chickens, indicating that laying rate, as a typical quantitative trait, exhibits pronounced phenotypic heterogeneity. These findings provide a reliable phenotypic basis for further investigation of the regulatory roles of ovary-related genes, such as *BMP15*, in the control of laying performance.

Figure 1 Statistics of egg *P*roduction of Huaixiang chickens aged 36–38 weeks

Figure 1. Comparison of egg production rate among high-, medium-, and low-laying Huaixiang chickens.

Egg production rate was significantly different among the three groups. Multiple comparisons showed extremely significant differences between all pairwise comparisons (****P < 0.0001). Bars represent the mean values of each group, and individual dots indicate data from individual hens.

Histological differences in follicular structure among laying performance groups

Histological observations revealed marked differences in follicular structure among Huaixiang chickens with different laying performances (Fig. 2). In the high-laying group, follicular tissues appeared relatively loose, with clear boundaries between the granulosa cell (GC) and theca cell (TC) layers and a moderate degree of tissue differentiation. In contrast, follicles from the low-laying group exhibited denser structures, accompanied by thickened or abnormally developed GC and TC layers, suggesting delayed follicular development or impaired function.

In large white follicles (LWF) (Fig. 2A–C), the high-laying group showed a relatively thinner TC layer and well-organized GC structure. With decreasing laying performance, both TC and GC layers gradually thickened and became more compact. Quantitative analysis demonstrated that TC thickness significantly increased as laying rate decreased ($P < 0.01$), with the highest value observed in the low-laying group. A similar trend was detected for GC thickness ($P < 0.05$ or $P < 0.01$). However, no significant difference in the TC/GC ratio was observed among groups ($P > 0.05$) (Fig. 2G-I).

In small yellow follicles (SYF) (Fig. 2D–F), the high- and medium-laying groups displayed well-developed GC layers with compact and orderly cell arrangement, whereas the low-laying group exhibited a markedly thinner and loosely organized GC layer. TC thickness showed only minor variation among groups. Quantitative analysis indicated that GC thickness in the low-laying group was extremely significantly reduced compared with the other groups ($P < 0.0001$), while the TC/GC ratio was significantly increased ($P < 0.01$) (Fig. 2J-L). Overall, these results suggest that GC layer development is closely associated with follicular maturation and laying performance in Huaixiang chickens.

Figure 2. Histological characteristics of large white follicles (LWF) and small yellow follicles (SYF) in Huaixiang chickens with different laying performances.

(A–C) Histological morphology of LWF in the high-, medium-, and low-laying groups. (D-F) Histological morphology of SYF in the high-, medium-, and low-laying groups. (G-I) Quantitative analysis of TC thickness, GC thickness, and TC/GC thickness ratio in LWF. (J-L) Quantitative analysis of TC thickness, GC thickness, and TC/GC thickness ratio in SYF.

TC, theca cell layer; GC, granulosa cell layer; OC, oocyte; CC, cavity structure. Scale bar = 100 μm. Data are presented as mean ± SEM. Significant differences are indicated as follows: *P < 0.05, **P < 0.01, ***P < 0.001, and ****P < 0.0001; ns, not significant.

Differential BMP15 expression in follicular tissues among laying performance groups

Semi-quantitative RT-PCR analysis demonstrated that *BMP15* was expressed in follicular tissues of Huaixiang chickens with different laying performances, with clear and specific amplification bands obtained using *β-actin* as the internal reference gene (Figs. 3A□B). Gray-scale analysis further revealed differences in the relative expression levels of *BMP15* among groups, showing an overall trend of highest expression in the high-laying group and lowest expression in the low-laying group (Figs. 3a□b).

As shown in Figs. 3a□b, *BMP15* expression patterns differed among follicular developmental stages. In large white follicles (LWF), the relative expression level of *BMP15* in the high-laying group was significantly higher than that in the low-laying group ($P < 0.05$), whereas the medium-laying group showed intermediate expression levels with no significant difference compared with either the high- or low-laying groups ($P > 0.05$). In contrast, more pronounced differences were observed in small yellow follicles (SYF). The high-laying group exhibited significantly higher *BMP15* expression than the low-laying group ($P < 0.01$), and the medium-laying group also showed significantly higher expression than the low-laying group ($P < 0.05$), while no significant difference was detected between the high- and medium-laying groups ($P > 0.05$).

Figure 3. Expression analysis of the *BMP15* gene in follicles of Huaixiang chickens with different laying performances.

(A) Semi-quantitative RT-PCR bands of *BMP15* expression in large white follicles (LWF) from high-, medium-, and low-laying groups. (B) Semi-quantitative RT-PCR bands of *BMP15* expression in small

yellow follicles (SYF) from high-, medium-, and low-laying groups. (a) Relative expression levels of *BMP15* in LWF among different laying-performance groups. (b) Relative expression levels of *BMP15* in SYF among different laying-performance groups.

β-actin was used as the internal reference gene. Data are presented as mean ± SEM. Significant differences are indicated as follows: *P < 0.05, **P < 0.01; ns, not significant.

Correlation Analysis between Laying Rate and BMP15 Expression

To further clarify the relationship between *BMP15* expression and laying performance, Pearson correlation analysis was conducted between individual laying rate and the relative expression levels of *BMP15* in follicles at different developmental stages (Fig. 4).

The results demonstrated that *BMP15* expression in both large white follicles (LWF) and small yellow follicles (SYF) was significantly positively correlated with laying rate (P < 0.01). Specifically, higher *BMP15* expression levels were associated with increased egg production. Overall, *BMP15* maintained a consistent positive relationship with laying performance throughout different stages of follicular development, suggesting that it may exert a continuous regulatory role during follicular growth and maturation. Combined with the observed expression patterns, these findings indicate that *BMP15* may influence laying performance by regulating granulosa cell proliferation and differentiation and promoting follicular maturation.

Figure 4 Correlation analysis between laying rate and *BMP15* expression in ovarian follicles of Huaixiang chickens.

Figure 4 Correlation analysis between laying rate and *BMP15* expression in follicles of Huaixiang chickens.

(A) Pearson correlation analysis between laying rate and *BMP15* relative expression in large white follicles (LWF). (B) Pearson correlation analysis between laying rate and *BMP15* relative expression in small yellow follicles (SYF).

Each dot represents an individual hen. Solid lines indicate linear regression trends. *BMP15* expression in both LWF and SYF showed significant positive correlations with laying rate (*P* < 0.01)

Phenotypic variation in egg shape index among Huaixiang chickens

Based on the measurements of egg shape index (SI), the experimental population was classified into three groups: the spherical egg group (SI > 75%), the standard-shaped egg group (70% ≤ SI ≤ 75%), and the elongated egg group (SI < 70%). The descriptive statistics of SI for each group are presented in Fig. 5.

The results indicated that significant differences in SI were observed among the three egg shape groups. Specifically, the spherical egg group exhibited a significantly lower SI compared with the standard-

shaped egg group ($P < 0.05$), and a highly significant lower SI compared with the elongated egg group ($P < 0.01$). In contrast, no significant difference was detected between the standard-shaped and elongated egg groups ($P > 0.05$). Overall, the SI showed an increasing trend from the spherical egg group to the elongated egg group.

Figure 5 Statistics of Egg shape index of Huaixiang chickens aged 36–38 weeks

Figure 5 Comparison of egg shape index among three egg shape categories.

The egg shape index (SI) was evaluated in eggs classified into three categories: elongated, normal, and ball-shaped. The box plots represent the mean SI values for each group, while individual data points illustrate the distribution of raw measurements.

Statistical significance (****, $P < 0.0001$) was assessed using one-way analysis of variance (ANOVA) followed by Tukey's multiple comparisons test.

Histological differences in oviduct magnum structure among egg shape formation groups

Histological observations revealed marked differences in the structural organization of the oviduct magnum among Huaixiang chickens with different egg shape indices (SI) (Fig. 6). Overall, mucosal fold morphology and glandular development exhibited a consistent pattern of variation associated with SI.

As shown in Fig. 6A–C, clear differences in mucosal fold architecture were observed among the three egg shape groups. The elongated egg group exhibited relatively broad and regularly arranged folds. In the normal egg group, fold width decreased, while branching complexity increased, resulting in a more intricate structure. In contrast, the ball-shaped egg group showed a pronounced increase in fold height with more prominent structural features.

Quantitative analysis (Fig. 6D–F) indicated that fold height in the ball-shaped egg group was significantly higher than in both the elongated and normal groups ($P < 0.0001$), and a significant difference was also observed between the elongated and normal groups ($P < 0.05$). For fold width, the normal group was significantly lower than the elongated group ($P < 0.05$), while no significant difference was found between the elongated and ball-shaped groups ($P > 0.05$). Additionally, the fold height-to-width ratio was significantly higher in the normal group compared with the elongated group ($P < 0.05$), with no significant differences among other comparisons ($P > 0.05$).

High-magnification observations (Fig. 7d-f) further revealed differences in epithelial and glandular structures. The ball-shaped egg group exhibited a thicker epithelial layer with well-developed tubular glands and stromal regions. The elongated group showed a looser architecture with more dispersed glands, whereas the normal group displayed an intermediate, more balanced tissue organization.

Figure 6 Histological characteristics of the oviductal ampulla in Huaixiang

chickens.

Figure 6 Morphological and quantitative analysis of oviducal mucosal folds in hens producing eggs of different shapes.

(A–C) Representative hematoxylin-eosin (HE)-stained photomicrographs of the oviduct magnum mucosa (100× magnification) from hens laying elongated (A), normal (B), and ball-shaped (C) eggs. Scale bars = 100 μm. (a-c) Higher-magnification images (400×) corresponding to the boxed regions in A–C, illustrating detailed structures of the mucosal folds. Abbreviations: E, epithelium; TG, tubular glands; S, stroma. Scale bars = 100 μm. (D-F) Quantitative analysis of mucosal fold height (D), width (E), and height-to-width ratio (F) among the three groups. Data are presented as mean ± standard error of the mean (SEM). Statistical significance was determined using one-way analysis of variance (ANOVA) followed by Tukey's multiple comparisons test. *$P < 0.05$, ****$P < 0.0001$; ns, not significant ($P > 0.05$).

Differential expression of ZDHHC2 Gene in the Oviduct Magnum among egg shape formation groups

As shown in Fig. 7, significant differences in *ZDHHC2* expression were observed in the oviduct magnum among the different egg shape index groups. The elongated egg group exhibited significantly higher *ZDHHC2* expression levels compared with the ball-shaped egg group ($P < 0.01$). Similarly, the normal egg group also showed significantly higher expression than the ball-shaped egg group ($P < 0.05$). However, no significant difference was detected between the elongated and normal egg groups ($P > 0.05$).

Figure 7 Expression analysis of *ZDHHC2* in the magnum of the oviduct from Huaixiang chickens at different laying stages.

Figure 7 Expression analysis of *ZDHHC2* mRNA in the oviduct of hens producing eggs of different shapes.

(A) Representative semi-quantitative RT-PCR gel electrophoresis results showing *ZDHHC2* and the reference gene *β-actin* in oviduct samples from hens producing elongated, normal, and ball-shaped eggs. (B) Quantitative analysis of relative *ZDHHC2* mRNA expression levels normalized to *β*-actin. Data are presented as mean ± standard error of the mean (SEM).

Statistical significance was evaluated using one-way analysis of variance (ANOVA) followed by Tukey's multiple comparisons test. *$P < 0.05$, **$P < 0.01$; ns, not significant ($P > 0.05$).

Correlation analysis between egg shape index and ZDHHC2 expression level

To further investigate the relationship between *ZDHHC2* gene expression and egg shape index (SI), Pearson correlation analysis was performed between SI and the relative expression level of *ZDHHC2* in the oviduct magnum (Fig. 8). The results demonstrated a significant positive correlation between *ZDHHC2* relative expression and SI ($P < 0.01$), indicating that the egg shape index increased with elevated *ZDHHC2* expression levels.

Figure 8 Correlation analysis between egg shape index and *ZDHHC2* expression in the magnum of oviduct in Huaixiang chickens.

Figure 8 Correlation analysis between egg shape index and relative *ZDHHC2* mRNA expression.

The scatter plot illustrates the linear relationship between egg shape index (x-axis) and relative *ZDHHC2* mRNA expression levels (y-axis). The solid red line represents the fitted linear regression line. The coefficient of determination (R^2) and statistical significance are indicated in the figure.

The results demonstrated a significant negative correlation between egg shape index and *ZDHHC2* mRNA expression ($P < 0.01$).

Discussion

Follicular structure and BMP15 expression in regulating laying performance

The process of follicular development is a central component in the formation of egg-laying performance in poultry, and its essence lies in the dynamic interactions between oocytes and surrounding somatic cells, particularly granulosa cells and theca cells (Onagbesan et al. 2009). A substantial body of research has demonstrated that follicular growth, selection, and ovulation are highly finely regulated processes, jointly governed by endocrine, paracrine, and autocrine factors (Chen et al. 2020; Nie et al. 2022). In this study, the integration of histological and molecular analyses further confirmed the important roles of follicular structural status and *BMP15* expression in the regulation of egg production (Elis et al. 2007).

Follicular structure serves as a direct indicator of developmental status and functional activity. Previous studies have shown that the coordinated development of the granulosa cell layer and the theca cell layer is crucial for maintaining normal follicular function (Gilbert et al. 1983; Pan et al. 2013). In the present study, follicles in the high-yield group exhibited relatively loose organization with moderately developed cellular layers, whereas those in the low-yield group showed a denser structure with significantly thickened theca and granulosa layers. These findings are consistent with those reported in other studies on follicular development in chickens (Du et al. 2022). The above observations suggest that follicular structure is not simply a case of “the thicker, the better,” but rather requires an appropriate tissue architecture to ensure efficient material exchange and signal transduction.

At the large white follicle (LWF) stage, follicles are in a phase of rapid growth, and their structural changes primarily reflect the level of cellular proliferation. Studies have shown that excessive proliferation or tightly packed cellular organization may lead to insufficient vascularization within the follicle, thereby impairing the supply of nutrients (Onagbesan et al. 2009; Kim et al. 2016; Yang et al. 2021). In the present study, the dense follicular structure observed in the low-yield group may restrict the diffusion of hormones and nutrients, consequently reducing follicular developmental efficiency (Stephens and Johnson 2017).

At the small yellow follicle (SYF) stage, follicles enter a critical period of selection and differentiation. In this study, the granulosa cell (GC) layer in the low-yield group was significantly thinner, accompanied by an increased TC/GC ratio, indicating impaired granulosa cell development. Previous studies have demonstrated that granulosa cells are not only the primary source of estrogen synthesis but also participate in follicular selection through the secretion of multiple growth factors, such as IGFs and BMPs (Johnson 2014). When GC development is compromised, follicular responsiveness to gonadotropins decreases, making follicles more susceptible to atresia (Hrabia et al. 2011). This finding is consistent with recent research showing that in atretic follicles, the proliferation of granulosa cells and their capacity for estradiol synthesis are significantly reduced.

Furthermore, this study found that changes in TC and GC thickness were synchronized at the LWF stage, whereas their ratio changed significantly at the SYF stage. This is consistent with the findings of (Nie et al. 2022)regarding structural remodeling during follicular selection, further indicating that the SYF stage plays a critical role in the regulation of egg production. Taken together, follicular structural alterations, particularly GC layer development, represent an important determinant of laying performance (Zhang et al. 2021).

BMP15, a member of the transforming growth factor-β (TGF-β) superfamily, is an oocyte-derived regulatory factor that plays a crucial role in follicular development (Otsuka et al. 2000; McNatty et al. 2004). Previous studies have demonstrated that BMP15 is widely expressed in avian ovaries and exhibits dynamic expression patterns across different stages of follicular development (Elis et al. 2007; Stephens and Johnson 2016). In the present study, *BMP15* was detected in the follicles of Huai Xiang chickens, with significantly higher expression in the high-yield group compared with the low-yield group, and it showed a significant positive correlation with laying rate. This finding is consistent with the reports of (Cael 2015)and (Wen et al. 2020), indicating that *BMP15* expression levels are positively associated with egg production performance. In addition, *BMP15* gene polymorphisms have been reported to be significantly associated with traits such as egg production and egg weight (Batista et al. 2013), further supporting its potential as a candidate gene.

In terms of its mechanism of action, *BMP15* primarily exerts its effects by regulating granulosa cell function. It has been shown that *BMP15* promotes granulosa cell proliferation, inhibits premature luteinization, and regulates steroid hormone synthesis (Otsuka and Shimasaki 2002; Shimasaki et al. 2004). Moreover, *BMP15* enhances granulosa cell sensitivity to follicle-stimulating hormone (FSH) via the SMAD signaling pathway, thereby promoting follicular development (Moore et al. 2003; Gilchrist et al. 2008). When *BMP15* expression is reduced, granulosa cell function is impaired, follicular development is disrupted, and ovulation rate decreases (Gilchrist et al. 2004).

From a developmental stage perspective, this study found that the expression difference of *BMP15* in small yellow follicles (SYF) was greater than that in large white follicles (LWF), which is consistent with transcriptomic studies suggesting that *BMP15* plays a more critical role during the follicular selection stage (Soglia et al. 2019). In addition, higher *BMP15* expression in small follicles contributes to follicular

recruitment and early development (Elis et al. 2007). Notably, by integrating *BMP15* expression with follicular structural changes, we observed a consistent association between *BMP15* levels and granulosa cell layer development, suggesting that *BMP15* may indirectly influence egg production by regulating GC layer development. This finding aligns with the “oocyte–granulosa cell regulatory axis” theory proposed by (Gilchrist et al. 2008).

Magnum structure and ZDHHC2 expression in regulating egg shape formation

Egg shape is a key component of egg quality in poultry, and its formation is coordinately regulated by different functional regions of the oviduct. Among these, the magnum plays a central role as the primary site of egg white secretion and is therefore critically involved in shaping the egg. Previous studies have demonstrated that egg shape is not only influenced by the initial morphology of the yolk, but is also closely associated with the rate of albumen deposition within the oviduct, mucosal structural characteristics, and luminal dynamics (Nys et al. 2004; Hincke et al. 2012). In this study, the role of the magnum in egg shape formation was analyzed from both histological and gene expression perspectives.

The structural characteristics of the magnum mucosa directly influence the mode of albumen secretion and deposition, thereby contributing to egg morphology to a certain extent. The present results showed significant differences in mucosal folding morphology and glandular development of the magnum among Huai Xiang chickens with different egg shape indices. Specifically, the round-egg group exhibited higher mucosal folds and more developed epithelial and glandular structures, whereas the long-egg group showed relatively looser tissue architecture (Nys et al. 2004).

Previous studies have indicated that the height and branching complexity of magnum mucosal folds directly determine the secretory surface area and the rate of albumen deposition. Well-developed fold structures increase albumen secretion, promoting a more uniform distribution of egg contents along both the longitudinal and transverse axes, thereby resulting in a more rounded egg shape (Hincke et al. 2012). In contrast, when mucosal folds are relatively simple or unevenly distributed, directional differences in albumen deposition may occur, potentially leading to elongated eggs. In the present study, the significantly increased fold height observed in the round-egg group supports this view. In addition, the development level of oviduct glands also plays an important role in egg shape formation. It has been reported that tubular glands in the magnum secrete large amounts of proteins, mainly ovalbumin, and that their secretory activity is closely related to albumen viscosity and spatial distribution (Yin et al. 2015). In this study, the more developed glandular structures observed in the round-egg group suggest stronger albumen secretion capacity, which may facilitate the formation of a more uniform albumen layer and thus stabilize egg shape proportions.

From a biomechanical perspective, during egg transport through the oviduct, the egg is subjected to both luminal contractions and the spatial distribution of its internal contents. When the magnum structure is well developed, it may help regulate the rhythm of albumen deposition and transport, promoting a more

balanced distribution of forces along both axes of the egg, thereby resulting in standard or round eggs. Conversely, when the structure is relatively underdeveloped, insufficient transverse support during longitudinal elongation may contribute to the formation of long eggs.

ZDHHC2 belongs to the DHHC family of palmitoyltransferases and is primarily involved in protein S-palmitoylation, playing important roles in regulating protein localization, stability, and signal transduction (E and J 2007; Globa and Bamji 2017). Although studies on *ZDHHC2* in the avian oviduct remain limited, its potential role in secretory function and epithelial regulation has received increasing attention (Greaves and Chamberlain 2011).

In the present study, *ZDHHC2* was differentially expressed in the magnum and showed a significant positive correlation with egg shape index, suggesting that it may be involved in regulating egg shape formation (Aicart-Ramos et al. 2011). Based on previous studies, *ZDHHC2* can regulate the palmitoylation of membrane and secretory proteins, thereby affecting their membrane localization and function (Rodriguez-Boulan and Macara 2014). In the magnum, this process may be closely associated with protein secretion, epithelial cell polarity maintenance, and secretory activity.

Functionally, *ZDHHC2* may participate in egg shape regulation through several potential pathways. First, by modulating the post-translational modification and trafficking of secretory proteins, it may influence the efficiency and spatial distribution of albumen secretion, thereby altering deposition patterns of egg contents. Second, by regulating epithelial membrane structure and signaling pathways, it may affect the formation and maintenance of mucosal folds in the oviduct. Third, it may be involved in cell–cell junctions and cytoskeletal remodeling processes, thereby influencing the local biomechanical environment of the oviduct (E and J 2007; Greaves and Chamberlain 2011). In addition, the observed positive correlation between *ZDHHC2* expression and egg shape index suggests a potentially promotive role in egg shape formation. Although direct functional validation is currently lacking, previous studies have demonstrated that post-translational protein modifications play essential roles in regulating membrane trafficking and glandular secretory activity (Resh 2013), thereby providing theoretical support for the potential involvement of *ZDHHC2* in this process.

In conclusion, *ZDHHC2* may indirectly influence egg shape formation by regulating protein secretion and the structural and functional characteristics of the oviduct epithelium, thereby participating in the determination of egg shape traits. This gene may serve as a novel candidate gene associated with egg shape characteristics; however, its precise mechanisms require further functional validation.

Conclusion

This study demonstrated that laying performance and egg shape traits in Huaiyang chickens are jointly regulated by ovarian and oviductal functions. *BMP15* expression was positively correlated with laying performance and was associated with follicular development, indicating its important role in ovarian regulation. In the oviduct magnum, structural differences in mucosal folds and glands were observed

among egg shape groups, while *ZDHHC2* expression showed a significant positive correlation with egg shape index, suggesting its involvement in egg shape formation through albumen secretion.

Declarations

Declaration of competing interest

The authors declare that they have no known competing financial interests or personal relationships that could have appeared to influence the work reported in this paper.

Funding

This work was supported by the National Natural Science Foundation of China (32472893-L.Z.) and the Natural Science Support Program Project of the Xinjiang Pro-duction and Construction Corps (2024DA006-J.W.).

Author contributions

Conceptualization, J.W. and L.Z.; validation, S.Y. and Q.L.; data curation, S.Y., Q.L. and X.Z.; writing-original draft preparation, S.Y. and Q.L.; writing-review and editing, S.Y., J.W. and L.Z.

Data availability statement

The datasets created or analyzed in our study are available from the corresponding author upon reasonable request.

References

1. Aicart-Ramos C, Valero RA, Rodriguez-Crespo I (2011) Protein palmitoylation and subcellular trafficking. Biochim Biophys Acta (BBA) - Biomembr 1808:2981–2994. https://doi.org/10.1016/j.bbamem.2011.07.009
2. Batista AM, Silva DMF, Rêgo MJBM, et al (2013) The expression and localization of leptin and its receptor in goat ovarian follicles. Anim Reprod Sci 141:142–147. https://doi.org/10.1016/j.anireprosci.2013.08.007
3. Cael BB (2015) The good, the bad, and the tiny: a simple, mechanistic-probabilistic model of virus-nutrient colimitation in microbes. PLOS One 10:e0143299. https://doi.org/10.1371/journal.pone.0143299

4. Chen Q, Wang Y, Liu Z, et al (2020) Transcriptomic and proteomic analyses of ovarian follicles reveal the role of VLDLR in chicken follicle selection. BMC Genomics 21:486. https://doi.org/10.1186/s12864-020-06855-w
5. Chen Y, Yu S, Zhang L, et al (2023) Effects and mechanisms investigation of heat stress on egg yolk quality in huaixiang chickens. Animals 13:. https://doi.org/10.3390/ani13223513
6. Du Y, Liu L, Liu Y, et al (2022) Ovary transcriptome profiling in high- and low-yielding chinese chahua laying chickens. Czech J Anim Sci 67:327–338. https://doi.org/10.17221/31/2022-CJAS
7. E LM, J DR (2007) Palmitoylation: policing protein stability and traffic. Nat Rev Mol Cell Biol 8:74–84. https://doi.org/10.1038/nrm2084
8. Elis S, Dupont J, Couty I, et al (2007) Expression and biological effects of bone morphogenetic protein-15 in the hen ovary. Expr biol eff bone morphog protein-15 hen ovary 194:485–497
9. Gilbert AB, Perry MM, Waddington D, Hardie MA (1983) Role of atresia in establishing the follicular hierarchy in the ovary of the domestic hen (*Gallus domesticus*). Reproduction 69:221–227. https://doi.org/10.1530/jrf.0.0690221
10. Gilchrist RB, Lane M, Thompson JG (2008) Oocyte-secreted factors: regulators of cumulus cell function and oocyte quality. Hum Reprod Update 14:159–177. https://doi.org/10.1093/humupd/dmm040
11. Gilchrist RB, Ritter LJ, Armstrong DT (2004) Oocyte–somatic cell interactions during follicle development in mammals. Anim Reprod Sci 82–83:431–446. https://doi.org/10.1016/j.anireprosci.2004.05.017
12. Globa AK, Bamji SX (2017) Protein palmitoylation in the development and plasticity of neuronal connections. Curr Opin Neurobiol 45:211–220. https://doi.org/10.1016/j.conb.2017.02.016
13. Greaves J, Chamberlain LH (2011) DHHC palmitoyl transferases: substrate interactions and (patho)physiology. Trends Biochem Sci 36:245–253. https://doi.org/10.1016/j.tibs.2011.01.003
14. Han H, Lei Q, Zhou Y, et al (2015) Association between BMP15 gene polymorphism and reproduction traits and its tissues expression characteristics in chicken. PLOS One 10:e0143298. https://doi.org/10.1371/journal.pone.0143298
15. Hincke MT, Nys Y, Gautron J, et al (2012) The eggshell: structure, composition and mineralization. Front Biosci-Landmark 17:1266–1280. https://doi.org/10.2741/3985
16. Hrabia A, Sechman A, Gertler A, Rząsa J (2011) Effect of growth hormone on steroid content, proliferation and apoptosis in the chicken ovary during sexual maturation. Cell Tissue Res 345:191–202. https://doi.org/10.1007/s00441-011-1187-5
17. Johnson AL (2014) The avian ovary and follicle development: some comparative and practical insights. Turk J Vet Anim Sci 38:661–669. https://doi.org/10.3906/vet-1405-6
18. Kim D, Lee J, Johnson AL (2016) Vascular endothelial growth factor and angiopoietins during hen ovarian follicle development. Gen Comp Endocrinol 232:25–31. https://doi.org/10.1016/j.ygcen.2015.11.017

19. McNatty KP, Moore LG, Hudson NL, et al (2004) The oocyte and its role in regulating ovulation rate: a new paradigm in reproductive biology. Reproduction 128:379–386. https://doi.org/10.1530/rep.1.00280
20. Mehta TN, Patel AK, Kulkarni GM, Suubbaiah G (2005) Determination of rosuvastatin in the presence of its degradation products by a stability-indicating LC method. J AOAC Int 88:1142–1147. https://doi.org/10.1093/jaoac/88.4.1142
21. Mishra B (2019) Genetic and hormonal regulation of egg formation in the oviduct of laying hens. Poult [Working Title]
22. Moore RK, Otsuka F, Shimasaki S (2003) Molecular basis of bone morphogenetic protein-15 signaling in granulosa cells *. J Biol Chem 278:304–310. https://doi.org/10.1074/jbc.M207362200
23. Moore RK, Shimasaki S (2005) Molecular biology and physiological role of the oocyte factor, BMP-15. Mol Cell Endocrinol 234:67–73. https://doi.org/10.1016/j.mce.2004.10.012
24. Narushin VG, Romanov MN (2002) Egg physical characteristics and hatchability. World's Poult Sci J 58:297–303. https://doi.org/10.1079/WPS20020023
25. Nie R, Zheng X, Zhang W, et al (2022) Morphological characteristics and transcriptome landscapes of chicken follicles during selective development. Anim: Open Access J MDPI 12:713. https://doi.org/10.3390/ani12060713
26. Nys Y, Gautron J, Garcia-Ruiz JM, Hincke MT (2004) Avian eggshell mineralization: biochemical and functional characterization of matrix proteins. CR Palevol 3:549–562. https://doi.org/10.1016/j.crpv.2004.08.002
27. Onagbesan O, Bruggeman V, Decuypere E (2009) Intra-ovarian growth factors regulating ovarian function in avian species: a review. Anim Reprod Sci 111:121–140. https://doi.org/10.1016/j.anireprosci.2008.09.017
28. Otsuka F, Shimasaki S (2002) A negative feedback system between oocyte bone morphogenetic protein 15 and granulosa cell kit ligand: its role in regulating granulosa cell mitosis. Proc Natl Acad Sci 99:8061–8065. https://doi.org/10.1073/pnas.122066899
29. Otsuka F, Yao Z, Lee T, et al (2000) Bone morphogenetic protein-15: IDENTIFICATION OF TARGET CELLS AND BIOLOGICAL FUNCTIONS *. J Biol Chem 275:39523–39528. https://doi.org/10.1074/jbc.M007428200
30. Pan X, Chen Z, Huang R, et al (2013) Transforming growth factor β1 induces the expression of collagen type I by DNA methylation in cardiac fibroblasts. PLOS One 8:e60335. https://doi.org/10.1371/journal.pone.0060335
31. Peşmen G (2025) Effect of egg shape index on hatching performance and gender. Turk J Agric Nat Sci 12:122–128. https://doi.org/10.30910/turkjans.1581699
32. Rangel PL, Rodríguez A, Gutiérrez K, et al (2014) Subdominant hierarchical ovarian follicles are needed for steroidogenesis and ovulation in laying hens (*Gallus domesticus*). Anim Reprod Sci 147:144–153. https://doi.org/10.1016/j.anireprosci.2014.04.011

33. Resh MD (2013) Covalent lipid modifications of proteins. Curr Biol 23:R431–R435. https://doi.org/10.1016/j.cub.2013.04.024
34. Robert JR (2004) Factors affecting egg internal quality and egg shell quality in laying hens. J Poult Sci 41:161–177. https://doi.org/10.2141/jpsa.41.161
35. Rodriguez-Boulan E, Macara IG (2014) Organization and execution of the epithelial polarity programme. Nat Rev Mol Cell Biol 15:225. https://doi.org/10.1038/nrm3775
36. Sah N, Kuehu DL, Khadka VS, et al (2021) RNA sequencing-based analysis of the magnum tissues revealed the novel genes and biological pathways involved in the egg-white formation in the laying hen. BMC Genomics 22:318. https://doi.org/10.1186/s12864-021-07634-x
37. Shimasaki S, Moore RK, Otsuka F, Erickson GF (2004) The bone morphogenetic protein system In mammalian reproduction. Endocr Rev 25:72–101. https://doi.org/10.1210/er.2003-0007
38. Soglia F, Silva AK, Tappi S, et al (2019) Gaping of pectoralis minor muscles: magnitude and characterization of an emerging quality issue in broilers. Poult Sci 98:6194–6204. https://doi.org/10.3382/ps/pez418
39. Stephens CS, Johnson PA (2017) Occludin expression and regulation in small follicles of the layer and broiler breeder hen. Gen Comp Endocrinol 248:106–113. https://doi.org/10.1016/j.ygcen.2017.02.010
40. Stephens CS, Johnson PA (2016) Bone morphogenetic protein 15 may promote follicle selection in the hen. Gen Comp Endocrinol 235:171–176. https://doi.org/10.1016/j.ygcen.2016.06.027
41. Todireanu C, Cotea C, Solcan C, Cornillie P (2014) Morphological aspects and differences between segments of the oviduct in chicken. Bull Univ Agric Sci Vet Med Cluj-Napoca, Vet Med 71:377–384. https://doi.org/10.15835/buasvmcn-vm:10502
42. Wang J, Liu Z, Cao D, et al (2023) Elucidation of the genetic determination of clutch traits in chinese local chickens of the laiwu black breed. BMC Genomics 24:686. https://doi.org/10.1186/s12864-023-09798-0
43. Wen D, Liu Y, Yu Q (2020) Metabolomic approach to measuring quality of chilled chicken meat during storage. Poult Sci 99:2543–2554. https://doi.org/10.1016/j.psj.2019.11.070
44. Yang D, Yang X, Dai F, et al (2021) The role of bone morphogenetic protein 4 in ovarian function and diseases. Reprod Sci 28:3316–3330. https://doi.org/10.1007/s43032-021-00600-8
45. Yin Y, Yang R, Han Y, Gu Z (2015) Comparative proteomic and physiological analyses reveal the protective effect of exogenous calcium on the germinating soybean response to salt stress. J Proteomics 113:111–126. https://doi.org/10.1016/j.jprot.2014.09.023
46. Zhang Q, Wang P, Cong G, et al (2021) Comparative transcriptomic analysis of ovaries from high and low egg-laying Lingyun black-bone chickens. Vet Med Sci 7:1867–1880. https://doi.org/10.1002/vms3.575

Figures

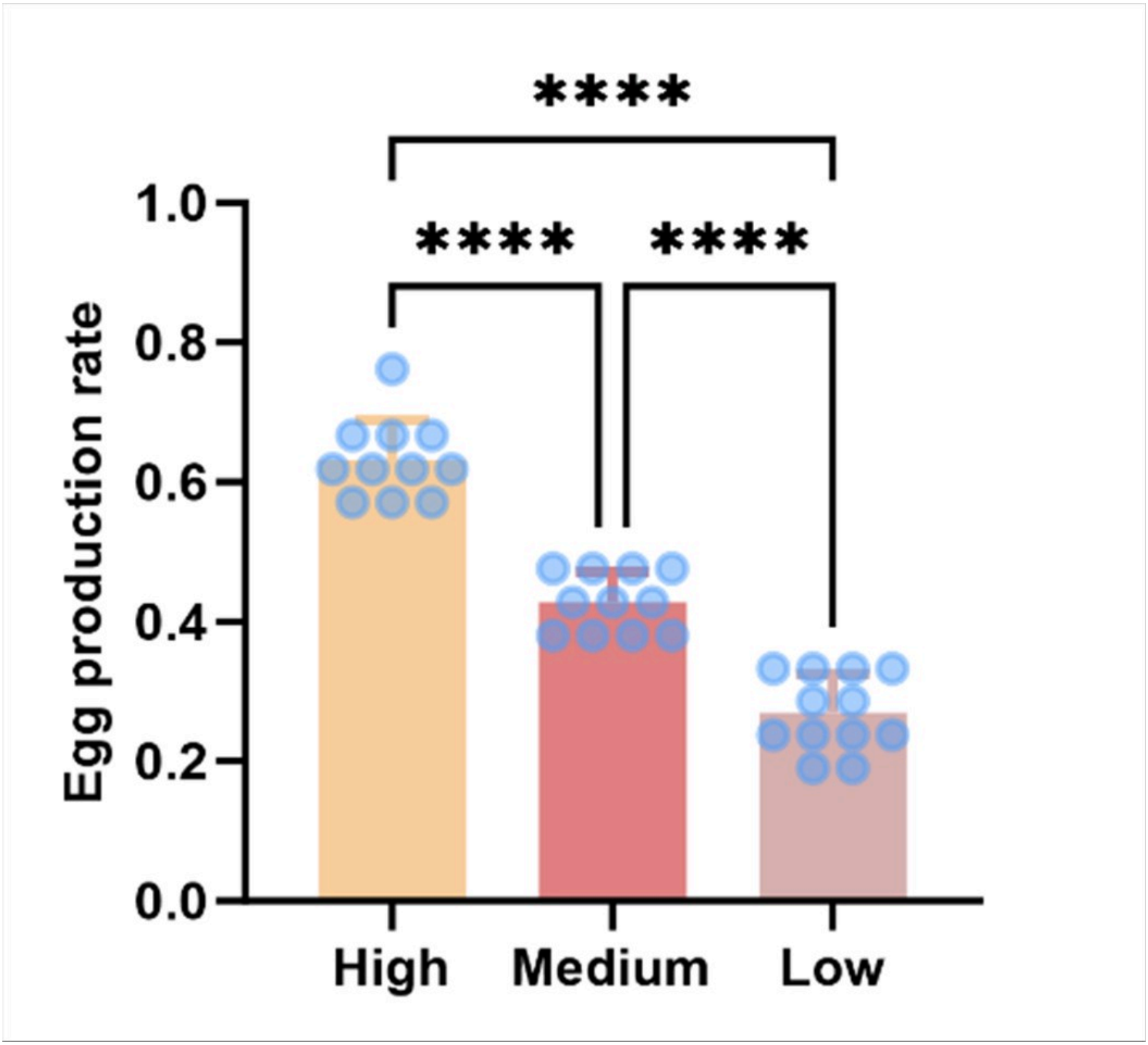


Figure 1

Statistics of egg *P*roduction of Huaixiang chickens aged 36-38 weeks

Fig. 1. Comparison of egg production rate among high-, medium-, and low-laying Huaixiang chickens.

Egg production rate was significantly different among the three groups. Multiple comparisons showed extremely significant differences between all pairwise comparisons (****P < 0.0001). Bars represent the mean values of each group, and individual dots indicate data from individual hens.

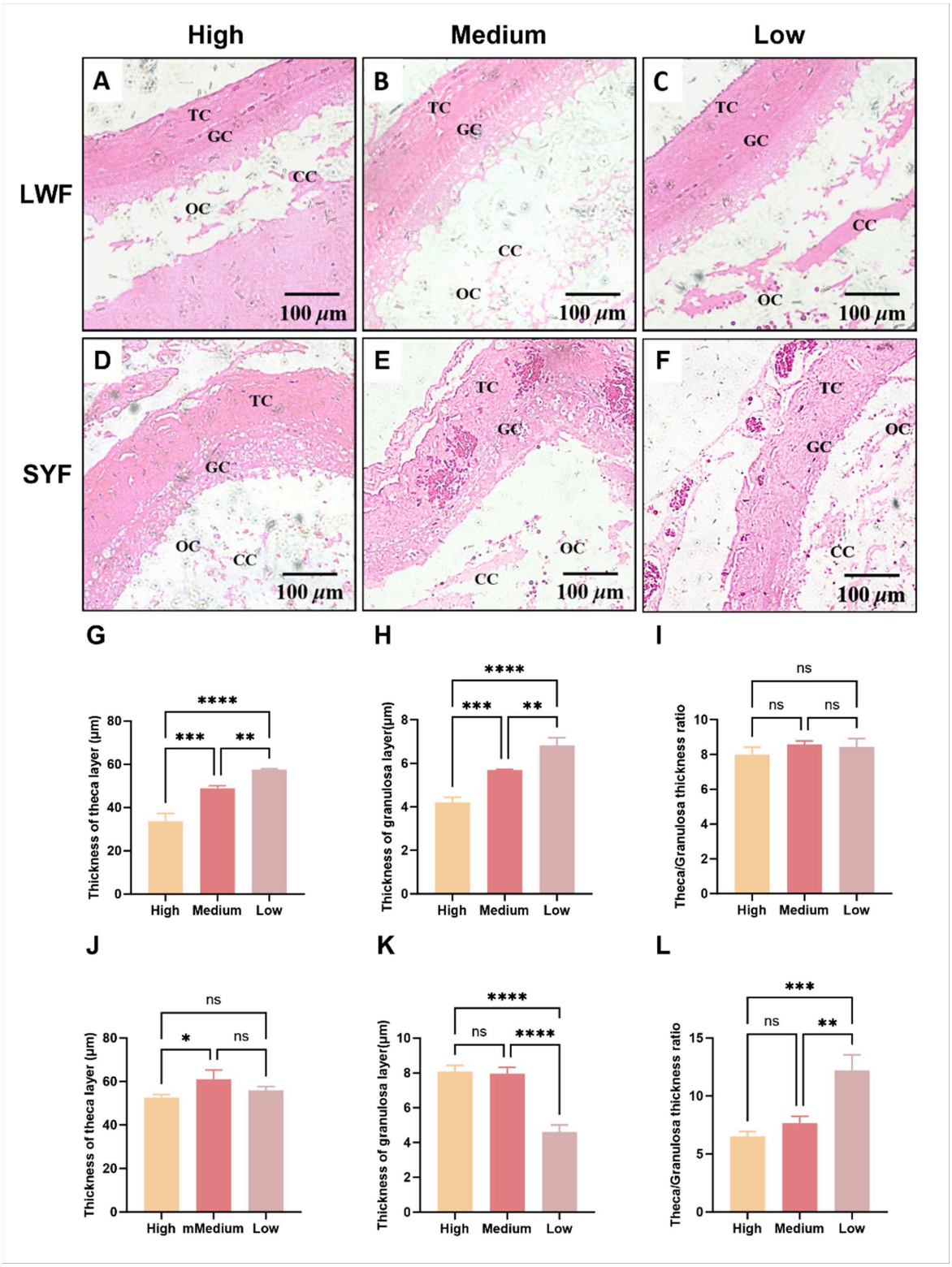


Figure 2

Histological characteristics of LWF and SYF in Huaixiang chickens.

Fig. 2. Histological characteristics of large white follicles (LWF) and small yellow follicles (SYF) in Huaixiang chickens with different laying performances.

(A–C) Histological morphology of LWF in the high-, medium-, and low-laying groups. (D-F) Histological morphology of SYF in the high-, medium-, and low-laying groups. (G-I) Quantitative analysis of TC thickness, GC thickness, and TC/GC thickness ratio in LWF. (J-L) Quantitative analysis of TC thickness, GC thickness, and TC/GC thickness ratio in SYF.

TC, theca cell layer; GC, granulosa cell layer; OC, oocyte; CC, cavity structure. Scale bar = 100 μm. Data are presented as mean ± SEM. Significant differences are indicated as follows: *P < 0.05, **P < 0.01, ***P < 0.001, and ****P < 0.0001; ns, not significant.

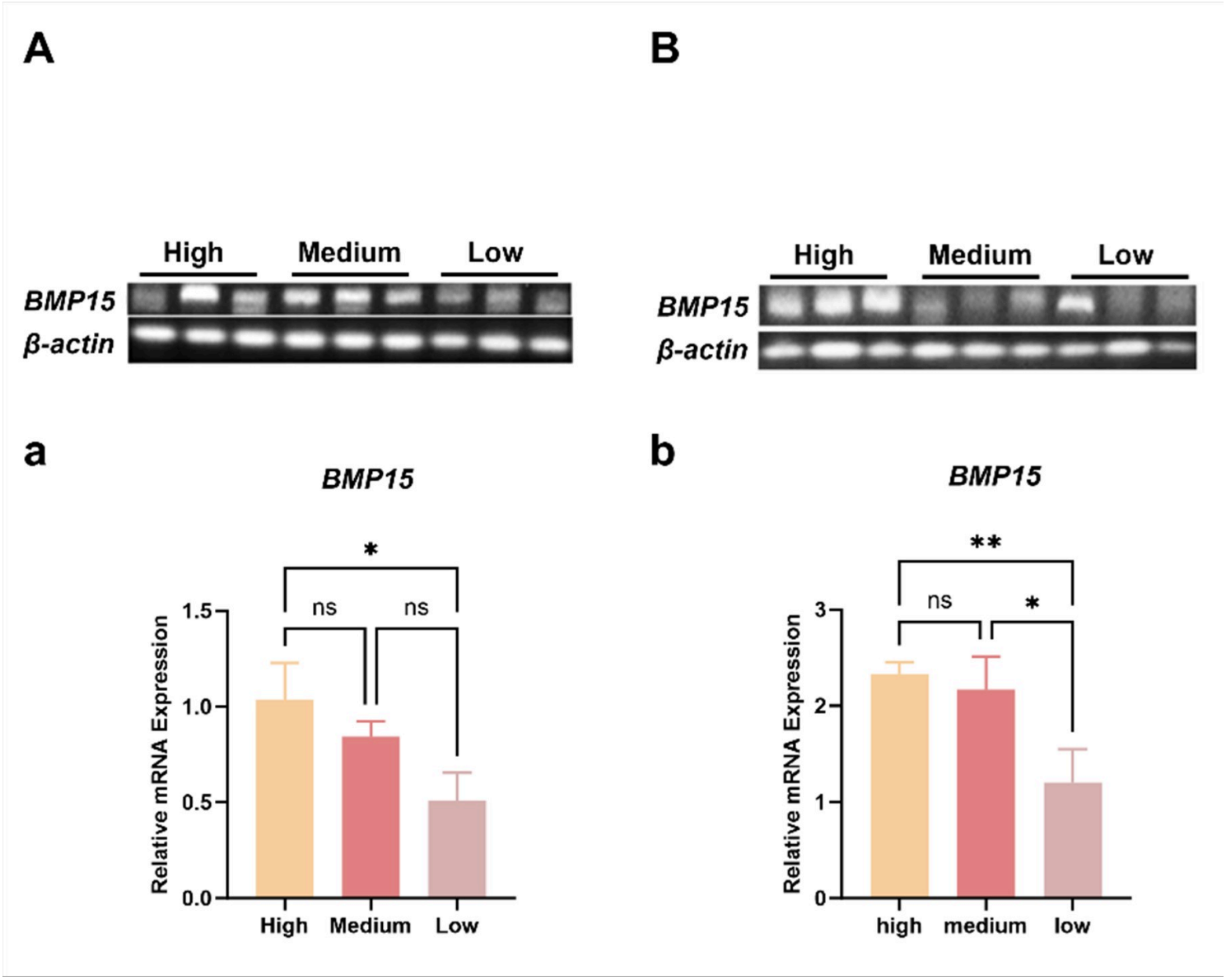


Figure 3

Expression analysis of *BMP15* in LWF and SYF of Huaixiang chickens at different laying stages.

Fig. 3. Expression analysis of the *BMP15* gene in follicles of Huaixiang chickens with different laying performances.

(A) Semi-quantitative RT-PCR bands of *BMP15*expression in large white follicles (LWF) from high-, medium-, and low-laying groups. (B) Semi-quantitative RT-PCR bands of *BMP15* expression in small yellow follicles (SYF) from high-, medium-, and low-laying groups. (a) Relative expression levels of *BMP15* in LWF among different laying-performance groups. (b) Relative expression levels of *BMP15* in SYF among different laying-performance groups.

β-actin was used as the internal reference gene. Data are presented as mean ± SEM. Significant differences are indicated as follows: *P < 0.05, **P < 0.01; ns, not significant.

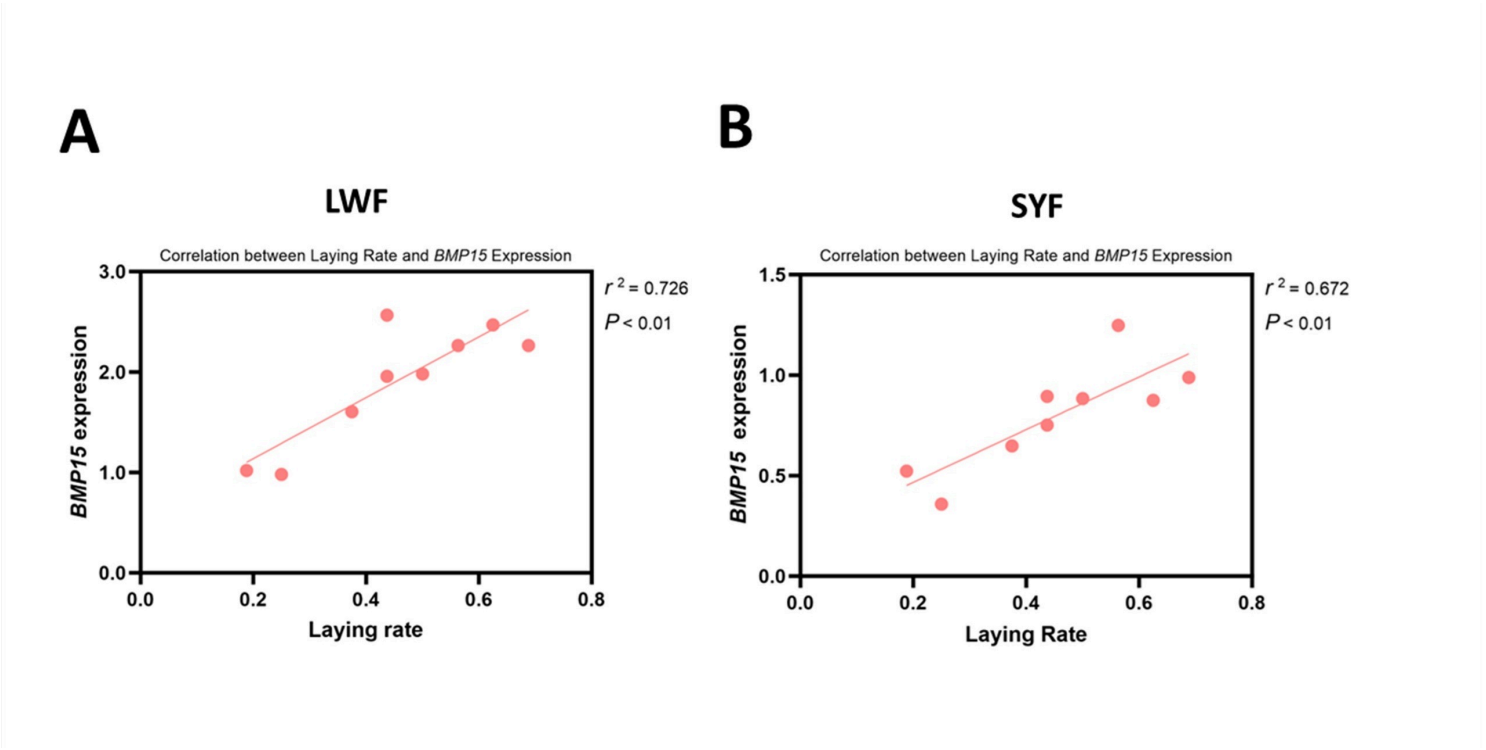


Figure 4

Correlation analysis between laying rate and *BMP15* expression in ovarian follicles of Huaixiang chickens.

Fig.4 Correlation analysis between laying rate and *BMP15*expression in follicles of Huaixiang chickens. (A) Pearson correlation analysis between laying rate and *BMP15* relative expression in large white follicles (LWF). (B) Pearson correlation analysis between laying rate and *BMP15* relative expression in small yellow follicles (SYF).

Each dot represents an individual hen. Solid lines indicate linear regression trends. *BMP15* expression in both LWF and SYF showed significant positive correlations with laying rate (*P* < 0.01)

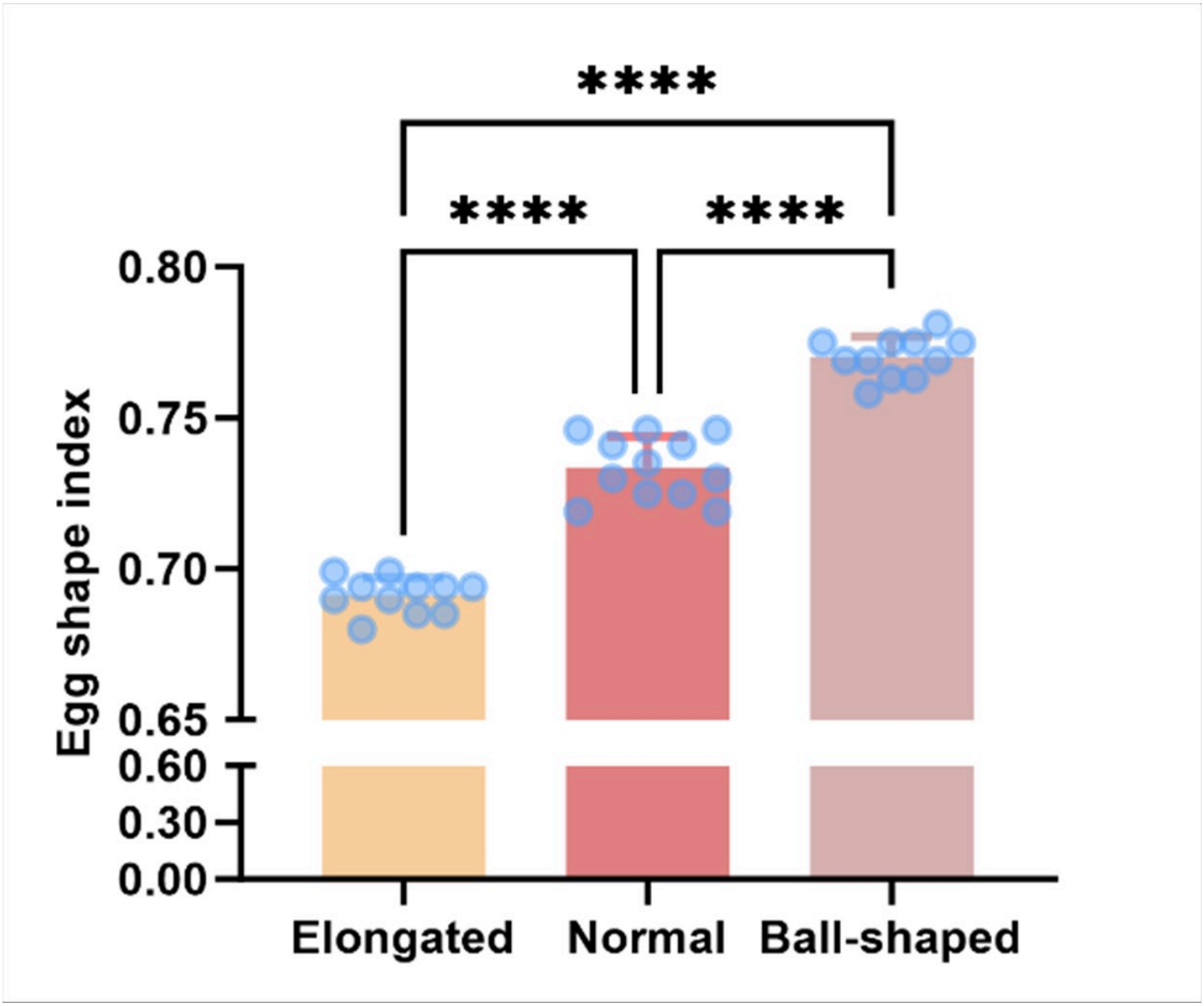


Figure 5

Statistics of Egg shape index of Huaixiang chickens aged 36-38 weeks

Fig.5 Comparison of egg shape index among three egg shape categories.

The egg shape index (SI) was evaluated in eggs classified into three categories: elongated, normal, and ball-shaped. The box plots represent the mean SI values for each group, while individual data points illustrate the distribution of raw measurements.

Statistical significance (****, $P < 0.0001$) was assessed using one-way analysis of variance (ANOVA) followed by Tukey's multiple comparisons test.

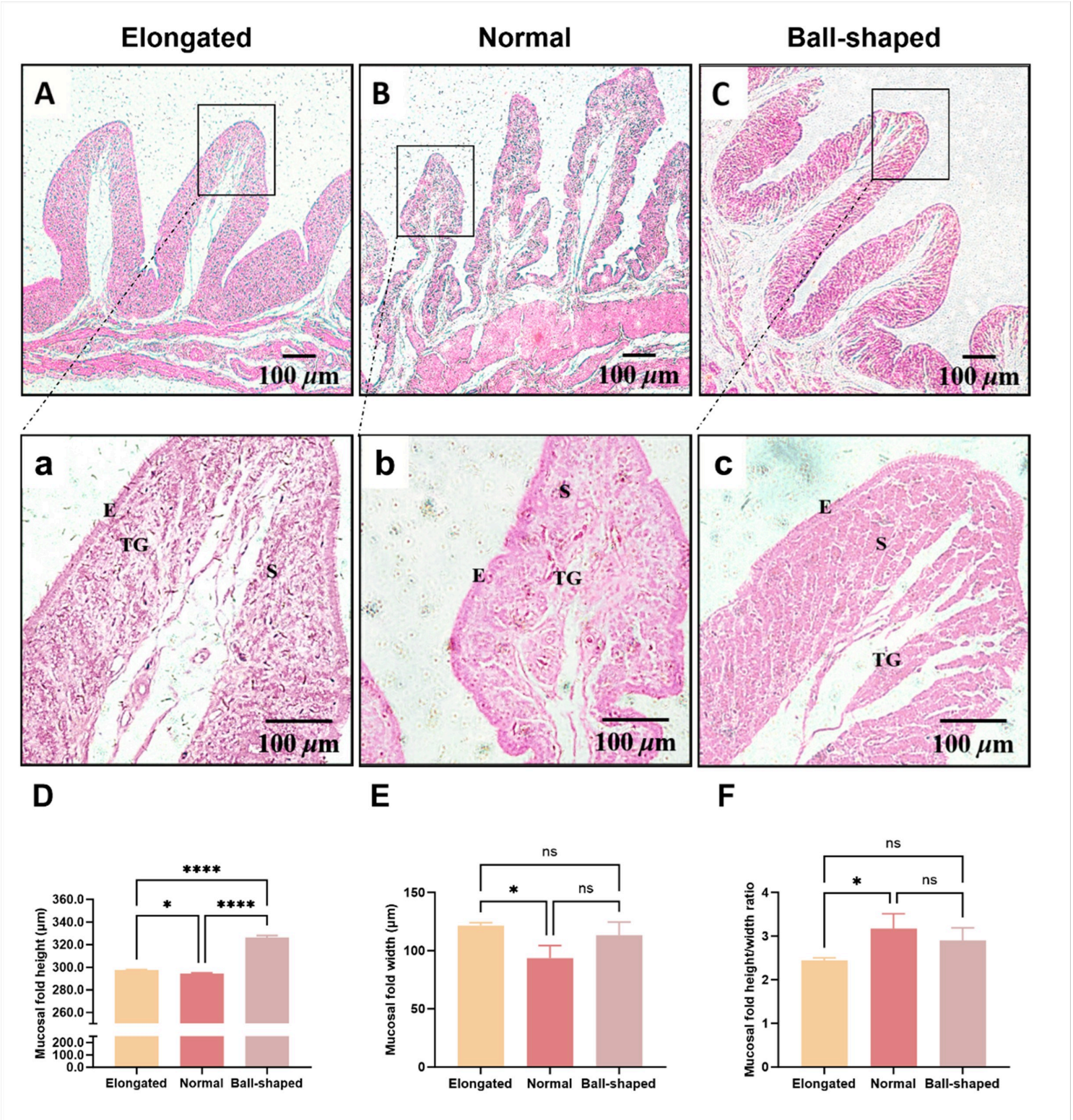


Figure 6

Histological characteristics of the oviductal ampulla in Huaixiang chickens.

Fig.6 Morphological and quantitative analysis of oviducal mucosal folds in hens producing eggs of different shapes.
(A–C) Representative hematoxylin-eosin (HE)-stained photomicrographs of the oviduct magnum mucosa (100× magnification) from hens laying elongated (A), normal (B), and ball-shaped (C) eggs. Scale bars = 100 μm. (a-c) Higher-magnification images (400×) corresponding to the boxed regions in A–C, illustrating detailed structures of the mucosal folds. Abbreviations: E, epithelium; TG, tubular glands; S, stroma. Scale bars = 100 μm. (D-F) Quantitative analysis of mucosal fold height (D), width (E), and height-to-width ratio (F) among the three groups. Data are presented as mean ± standard error of the mean (SEM). Statistical significance was determined using one-way analysis of variance (ANOVA) followed by Tukey's multiple comparisons test. *P < 0.05, ****P < 0.0001; ns, not significant (P> 0.05).

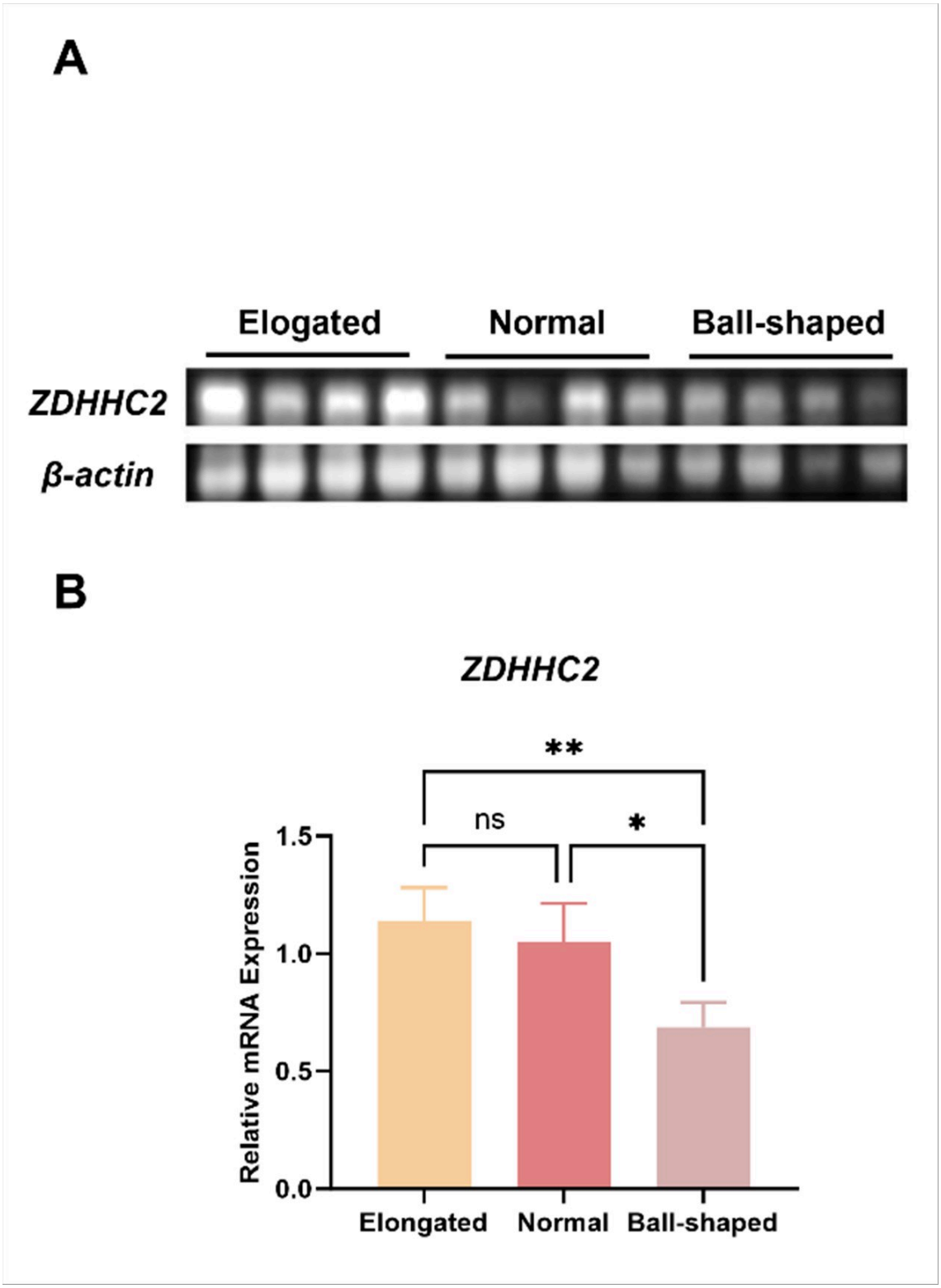


Figure 7

Expression analysis of *ZDHHC2* in the magnum of the oviduct from Huaixiang chickens at different laying stages.

Fig.7 Expression analysis of *ZDHHC2* mRNA in the oviduct of hens producing eggs of different shapes.

(A) Representative semi-quantitative RT-PCR gel electrophoresis results showing *ZDHHC2* and the reference gene *β-actin* in oviduct samples from hens producing elongated, normal, and ball-shaped eggs. (B) Quantitative analysis of relative *ZDHHC2* mRNA expression levels normalized to *β*-actin. Data are presented as mean ± standard error of the mean (SEM).

Statistical significance was evaluated using one-way analysis of variance (ANOVA) followed by Tukey's multiple comparisons test. **P* < 0.05, ***P* < 0.01; ns, not significant (*P* > 0.05).

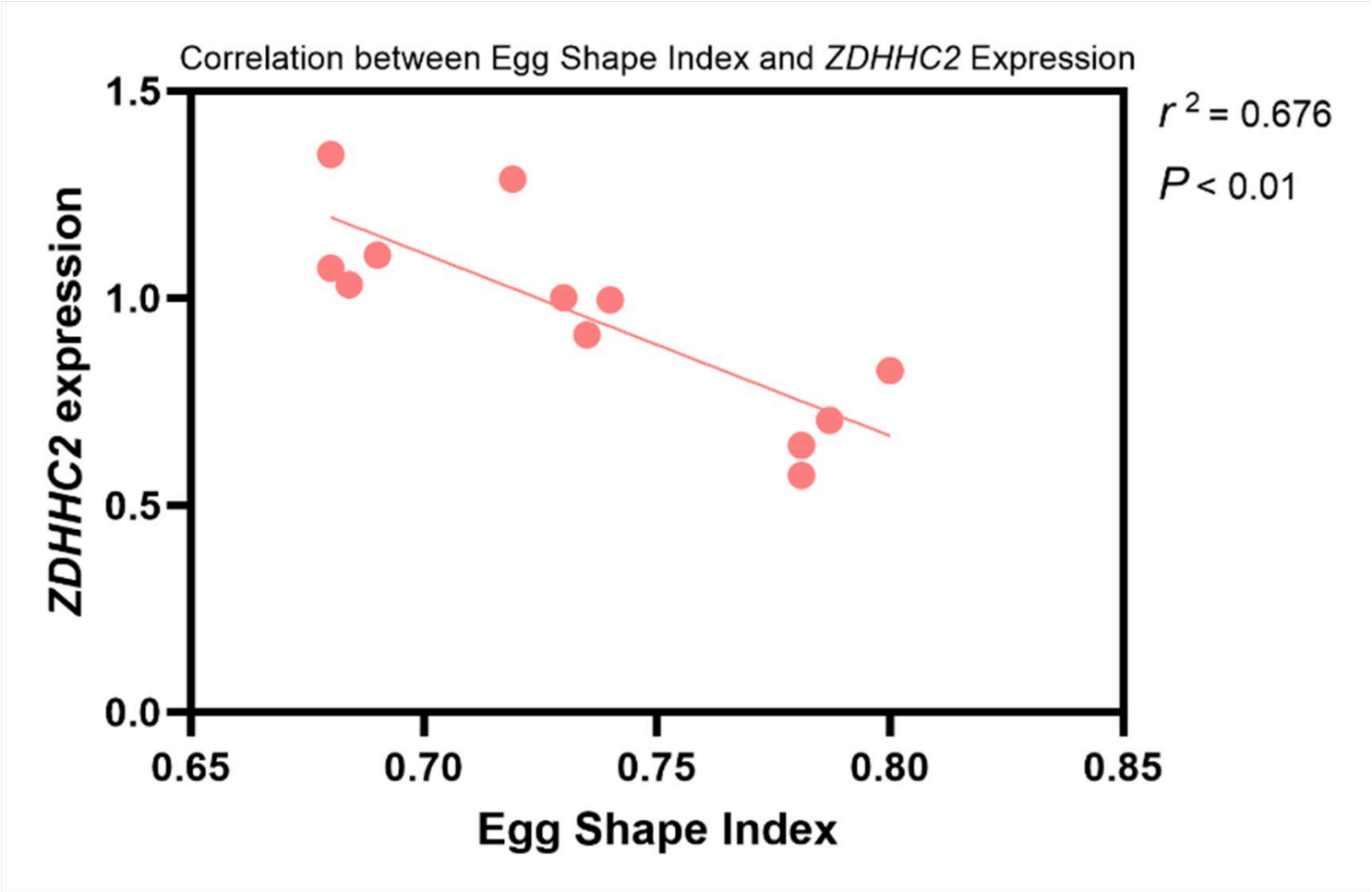


Figure 8

Correlation analysis between egg shape index and *ZDHHC2* expression in the magnum of oviduct in Huaixiang chickens.

Fig.8 Correlation analysis between egg shape index and relative *ZDHHC2* mRNA expression.

The scatter plot illustrates the linear relationship between egg shape index (x-axis) and relative *ZDHHC2* mRNA expression levels (y-axis). The solid red line represents the fitted linear regression line. The coefficient of determination (R^2) and statistical significance are indicated in the figure.

The results demonstrated a significant negative correlation between egg shape index and *ZDHHC2* mRNA expression (*P* < 0.01).